



DIGITAL ACCESS TO SCHOLARSHIP AT HARVARD

Atomic Layer Deposition of Sc_2O_3 for Passivating AlGaIn/GaN High Electron Mobility Transistor Devices

The Harvard community has made this article openly available.
[Please share](#) how this access benefits you. Your story matters.

Citation	Wang, Xinwei, Omair I. Saadat, Bin Xi, Xiabing Lou, Richard J. Molnar, Tomás Palacios, and Roy G. Gordon. 2012. Atomic layer deposition of Sc_2O_3 for passivating AlGaIn/GaN high electron mobility transistor devices. Applied Physics Letters 101: 232109.
Published Version	doi:10.1063/1.477071
Accessed	February 19, 2015 11:00:35 AM EST
Citable Link	http://nrs.harvard.edu/urn-3:HUL.InstRepos:10055799
Terms of Use	This article was downloaded from Harvard University's DASH repository, and is made available under the terms and conditions applicable to Other Posted Material, as set forth at http://nrs.harvard.edu/urn-3:HUL.InstRepos:dash.current.terms-of-use#LAA

(Article begins on next page)

Atomic layer deposition of Sc_2O_3 for passivating AlGaN/GaN high electron mobility transistor devices

Xinwei Wang,^{1,a)} Omair I. Saadat,^{2,a)} Bin Xi,¹ Xiabing Lou,¹ Richard J. Molnar,⁴ Tomás Palacios,² and Roy G. Gordon^{1,3}

¹Department of Chemistry and Chemical Biology, Harvard University, Cambridge, Massachusetts 02138, USA

²Department of Electrical Engineering and Computer Science, Massachusetts Institute of Technology, Cambridge, Massachusetts 02139, USA

³School of Engineering and Applied Sciences, Harvard University, Cambridge, Massachusetts 02138, USA

⁴Massachusetts Institute of Technology, Lincoln Laboratory, Lexington, Massachusetts 02420, USA

(Received 25 October 2012; accepted 15 November 2012; published online 7 December 2012)

Polycrystalline, partially epitaxial Sc_2O_3 films were grown on AlGaN/GaN substrates by atomic layer deposition (ALD). With this ALD Sc_2O_3 film as the insulator layer, the Sc_2O_3 /AlGaN/GaN metal-insulator-semiconductor high electron mobility transistors showed excellent electrical performance with a high $I_{\text{on}}/I_{\text{off}}$ ratio of over 10^8 and a low subthreshold slope of 75 mV/dec. The UV/ NH_4OH surface treatment on AlGaN/GaN prior to ALD was found to be critical for achieving these excellent figures. In addition, the Sc_2O_3 dielectric is found to be negatively charged, which facilitates the enhancement-mode operation. While bare Sc_2O_3 suffers from moisture degradation, depositing a moisture blocking layer of ALD Al_2O_3 can effectively eliminate this effect. © 2012 American Institute of Physics. [<http://dx.doi.org/10.1063/1.4770071>]

Gallium-nitride based high electron mobility transistors (HEMTs) are promising for high frequency switches and high power devices. However, typical AlGaN/GaN HEMTs rely on Schottky gates, which suffer from high gate leakage and impose a limit on the maximum gate bias that can be applied to the device. Applications for power electronics require low leakage in the off-state and large voltage swings, and thus it is necessary to fabricate devices with a gate dielectric, *i.e.*, metal-insulator-semiconductor (MIS)-HEMTs. Atomic layer deposition (ALD) of high- k dielectrics, such as HfO_2 and Al_2O_3 , is a promising technique for depositing gate dielectrics due to its precise control of the film thickness. These ALD oxides have very low leakage, and their high- k dielectric constant ensures an effective channel modulation by the gate, even with relatively large dielectric thickness. In addition, the accurate thickness control allowed by ALD enables ultra-smooth conformal films without pinholes.

Scandium oxide (Sc_2O_3) is another high- k oxide material that has also been reported to form a good gate dielectric for AlGaN/GaN MIS-HEMTs and to mitigate current collapse.¹ Sc_2O_3 has a dielectric constant of 14 and a band gap of 6.3 eV with high conduction and valence band offsets.² Crystalline Sc_2O_3 exists in a cubic bixbyite crystal structure with a mismatch of 9% in its (111) orientation parallel to the GaN (0001) plane. In early reports, the Sc_2O_3 was mainly prepared by molecular beam epitaxy (MBE) in a high-vacuum chamber, and a heteroepitaxy of Sc_2O_3 on GaN with a relationship of $(111) \times [1\bar{1}0]_{\text{Sc}_2\text{O}_3} // (0001) \times [11\bar{2}0]_{\text{GaN}}$ was achieved under certain growth conditions.³ The heteroepitaxy was considered to be beneficial for good electrical properties, as it tends to minimize the density of surface dangling bonds that could be a source for surface states on the GaN.

However, despite the high quality of MBE films, MBE is difficult to scale up due to cost and technical reasons. In this letter, we report promising electrical performance of ALD Sc_2O_3 thin films on AlGaN/GaN devices. These Sc_2O_3 films are partly epitaxial, polycrystalline films with some mis-oriented grains. The fabricated devices have excellent subthreshold slopes and high $I_{\text{on}}/I_{\text{off}}$ ratios. The proposed ALD of Sc_2O_3 dielectrics on GaN-based transistors is very promising, as it combines the excellent properties of Sc_2O_3 dielectrics with the large-scale of ALD equipment.⁴

The ALD of Sc_2O_3 was carried out in a home-built tubular reactor. Scandium tris(N,N' -diisopropylacetamidate) and H_2O were used as scandium and oxygen sources, respectively. The scandium precursor was kept in a sealed bubbler in an oven heated to 160 °C, and was delivered into the reaction chamber with N_2 carrier gas. Si(100) and (111) wafers were used for characterizing the Sc_2O_3 growth. Each Si wafer was treated with UV light for 5 min and then dipped into a dilute HF solution for 30 s before being loaded into the deposition chamber. The Sc_2O_3 deposition was performed at substrate temperatures from 300 °C to 360 °C. The growth rate was 0.03 nm/cycle at 300 °C, and increased to 0.07 nm/cycle at 360 °C. Detailed descriptions of the deposition process can be found in our previous report.⁵ Transmission electron microscopy (TEM) was used to examine the crystallinity of the as-deposited Sc_2O_3 films. As shown in Figure 1, the top-view and cross-sectional-view TEM images clearly show the polycrystalline structure of the Sc_2O_3 films deposited on a SiN_x TEM grid and a Si(111) substrate, respectively. The corresponding electron diffraction patterns (not shown here) matched well with the Sc_2O_3 bixbyite cubic phase. In addition, we noticed that epitaxial growth of Sc_2O_3 on Si (111) has been achieved by MBE,⁶ whereas polycrystalline films were deposited by our ALD method. This difference might be due to the formation of an ultra-thin layer of

^{a)}X. Wang and O. I. Saadat contributed equally to this work.

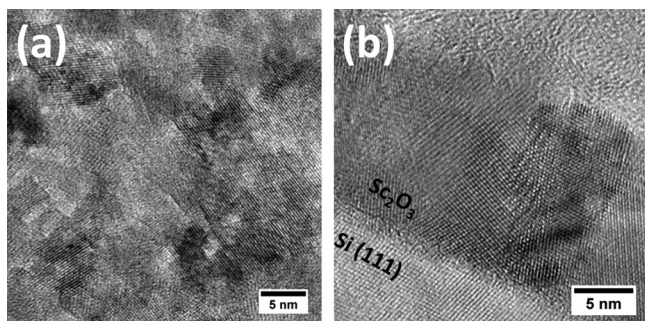


FIG. 1. (a) Top-view and (b) cross-sectional-view TEM images of the as-deposited Sc_2O_3 on an amorphous SiN_x TEM grid and a Si(111) substrate, respectively. Both show polycrystalline Sc_2O_3 grains.

SiO_2 during the initial growth,⁷ and a similar phenomenon was observed in ALD growth of LaLuO_3 on Si (111) in our previous studies.⁸

Sc_2O_3 was deposited on AlGaIn/GaN substrates, which were later processed into HEMT devices for characterizing the electrical and transport properties. The AlGaIn/GaN substrates were grown by metal-organic chemical vapor deposition (MOCVD) on sapphire single crystals, and the structure was composed of $0.8 \mu\text{m}$ of Fe-doped insulating GaN, $1.2 \mu\text{m}$ unintentionally doped GaN, 1 nm AlN, 17 nm AlGaIn (28% Al), and finally a 2 nm GaN capping layer. The cross-sectional TEM image in Figure 2(a) shows that a highly textured polycrystalline Sc_2O_3 film was grown on AlGaIn/GaN with a preferred growth orientation of (111). The majority of the Sc_2O_3 micro-grains were oriented in the direction $(111)_{\text{Sc}_2\text{O}_3} // (0001)_{\text{GaN}}$, *e.g.*, the highlighted grains “A” and “B” in Figure 2(a). There were also a few grains showing a tilted orientation, *e.g.*, the grain “C” in Figure 2(a). We also noticed that the slight difference in the lattice texture of the grains “A” and “B,” which suggested a relationship of in-plane rotation between the two grains. The TEM image also showed no observable interfacial layer between Sc_2O_3 and GaN. The preferred growth orientation was further examined by selective area electron diffraction (ED), as shown in Figure 2(b). Rather than diffraction rings, the ED pattern only shows scattered Sc_2O_3 diffraction spots, within which the spots with stronger intensity belong to $\text{Sc}_2\text{O}_3(222)$ and $(4-40)$. This again supported that the grains were highly oriented, and the preferred growth orientation had a relationship

of $(111) \times [1\bar{1}0]_{\text{Sc}_2\text{O}_3} // (0001) \times [11\bar{2}0]_{\text{GaN}}$ to the substrate. In addition, we also noticed a few relatively weak spots, circled in the ED pattern, that correspond to the misaligned micrograins as shown in the TEM image (Figure 2(a)).

$\text{Sc}_2\text{O}_3/\text{AlGaIn}/\text{GaN}$ MIS-HEMT devices were fabricated for characterizing the electrical properties. The HEMT devices were fabricated on the same AlGaIn/GaN substrate mentioned above. Ti/Al/Ni/Au ohmic metals were patterned, deposited, and annealed at 870°C to form ohmic source/drain contacts. Then, mesa isolation was performed by etching with a Cl_2/BCl_3 plasma before deposition of the gate dielectric. In order to study the effect of surface treatment before the Sc_2O_3 deposition, some of the devices were first exposed to UV in air for 5 min, and then immersed in NH_4OH (aqueous, 15%) for 10 min, while some other samples were only treated with UV.⁹ Then 20 nm of Sc_2O_3 was deposited on top of the device samples at a temperature of 330°C by 400 ALD cycles. After the Sc_2O_3 deposition, Ni/Au/Ni gates were deposited by e-beam evaporation and patterned by liftoff. Finally, the devices were annealed in forming gas at 400°C for 30 s in order to improve the subthreshold slope and $I_{\text{on}}/I_{\text{off}}$ behavior.¹⁰

Ambient moisture was found to have a noticeable impact on the electrical performance of the Sc_2O_3 devices as shown both in C-V (red curves in Figure 3) and I-V measurements (blue and green curves in Figure 4). Compared with the measured results in vacuum, the capacitance measured in air is higher and the threshold voltage is positively shifted. This is likely because the ambient water molecules diffuse through the grain boundaries of the Sc_2O_3 layer and reach the AlGaIn surface and these molecules respond to AC signals through a process of ionization and deionization.¹¹ Therefore, to avoid the effect of moisture, we performed our measurements in vacuum unless specified.

We also investigated the effect of the surface treatment of UV and UV/ NH_4OH on AlGaIn/GaN prior to the Sc_2O_3 deposition. Both UV and UV/ NH_4OH treated $\text{Sc}_2\text{O}_3/\text{AlGaIn}/\text{GaN}$ HEMTs showed excellent transfer characteristics: the $I_{\text{on}}/I_{\text{off}}$ ratio of over 10^8 and subthreshold slope of 75 mV/dec for the HEMTs with the NH_4OH treatment (Figure 4); while the HEMTs with the UV treatment showed slightly worse results with a subthreshold slope of 80 mV/dec and an $I_{\text{on}}/I_{\text{off}}$ ratio of 8×10^7 (not shown here). The electron mobility was

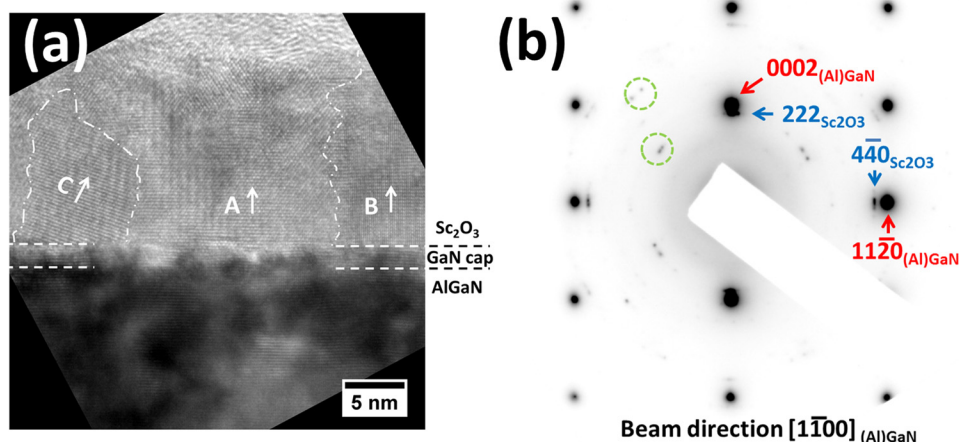


FIG. 2. (a) Cross-sectional TEM image of Sc_2O_3 grown on an AlGaIn/GaN substrate showing epitaxial $(111)_{\text{Sc}_2\text{O}_3} // (0001)_{\text{GaN}}$ grains A and B, and tilted grain C, and (b) the corresponding selective area electron diffraction pattern.

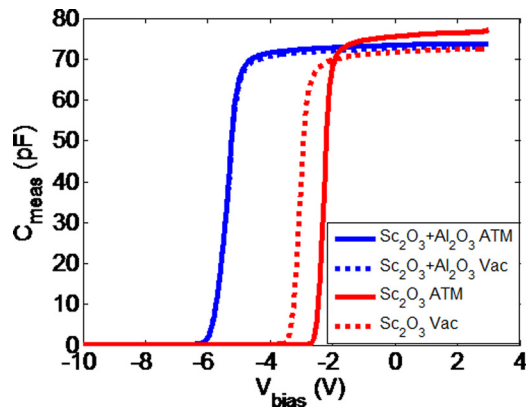


FIG. 3. 1 MHz C-V Measurements show that by adding Al_2O_3 on top of Sc_2O_3 , the differences between device behavior in atmosphere and vacuum are eliminated. C-V measurements at lower frequency (down to 100 Hz, not shown here) indicate that frequency dispersion can also be eliminated by either measuring in vacuum or adding an Al_2O_3 capping layer, which further confirms the impact of atmosphere on Sc_2O_3 . The hysteresis for the Sc_2O_3 capacitor measured in vacuum (not shown here) is around 50 mV, which is within the measurement limit.

determined to be $2050 \text{ cm}^2/\text{Vs}$, which is slightly higher than that of the AlGaIn/GaN Schottky HEMTs, *i.e.*, $2000 \text{ cm}^2/\text{Vs}$. The threshold voltage for transistors with Sc_2O_3 dielectric is lower than for other high- k dielectrics. Additionally, Q-point pulsed I-V measurements were performed on the Sc_2O_3 HEMTs with and without the NH_4OH treatment, and the results are shown in Figure 5. The devices with NH_4OH treatment showed much less current collapse compared with the devices with only UV treatment. These results suggest that the surface treatment of AlGaIn/GaN is crucial for obtaining good electrical properties, and the UV/ NH_4OH pretreatment provides a better quality of the interface between oxide and AlGaIn/GaN.

To prevent the effect from moisture, Gao *et al.* suggested adding a fluorocarbon layer as the moisture blocking layer.¹¹ Here, we propose adding a thin layer of ALD Al_2O_3 on top of the Sc_2O_3 as the moisture blocking layer, since ALD Al_2O_3 is known to have low water permeability.¹² We made capacitors with 10 nm Sc_2O_3 capped with 10 nm Al_2O_3 by *in situ* ALD. As the blue curves shown in Figure 3, the capacitors do not show any variation in 1 MHz C-V measurements whether in air or in vacuum. At the same time, the $I_{\text{on}}/I_{\text{off}}$ ratio remains almost the same (Figure 4). This shows that

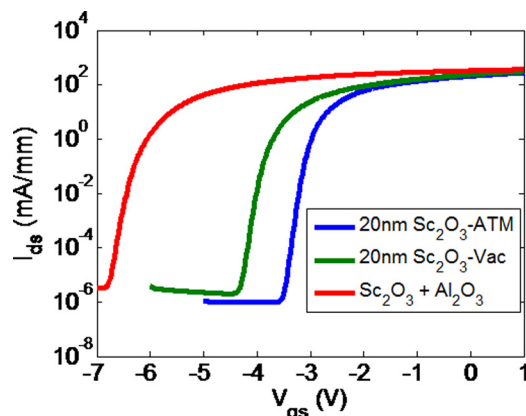


FIG. 4. Transfer characteristics show impact of moisture on Sc_2O_3 MIS-HEMTs. All devices have NH_4OH pretreatment ($V_{\text{ds}} = 10 \text{ V}$).

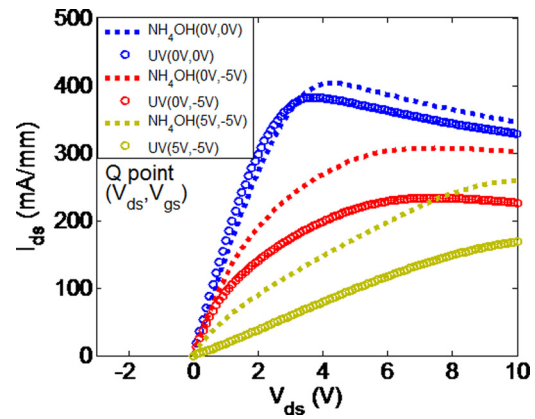


FIG. 5. Sc_2O_3 MIS-HEMTs with NH_4OH pre-treatment show less current collapse than MIS-HEMTs with just UV treatment. Current was measured 1 ms after switching from the Q-point.

the Sc_2O_3 surface can be effectively passivated by ALD Al_2O_3 . Q-point pulsed I-V measurements on $\text{Al}_2\text{O}_3/\text{Sc}_2\text{O}_3$ HEMTs show almost the same results as Sc_2O_3 HEMTs, suggesting that the quality of the interface between Sc_2O_3 and AlGaIn/GaN, rather than the top surface of Sc_2O_3 , is the main determinant of the current collapse behavior. In addition, by integrating the 1 MHz C-V curves (Figure 6), one can obtain the carrier concentration in the channel. The Sc_2O_3 dielectric layer was found to be effective in helping to deplete carriers in the channel, which is necessary for enhancement-mode operation, while adding Al_2O_3 under the gate can increase the carrier concentration. This allows for reducing the carrier concentration from $8 \times 10^{12} \text{ cm}^{-2}$ with pure Al_2O_3 to $5 \times 10^{12} \text{ cm}^{-2}$ with pure Sc_2O_3 on a HEMT structure that has a carrier concentration of $6.5 \times 10^{12} \text{ cm}^{-2}$ without any gate oxide, resulting in reduced turn-on voltages. Coupled with the excellent subthreshold slope and high $I_{\text{on}}/I_{\text{off}}$ ratio, Sc_2O_3 based oxides are very promising for AlGaIn/GaN HEMTs for power applications.

In summary, we found that polycrystalline, partially epitaxial Sc_2O_3 films on GaN can be grown by ALD. This Sc_2O_3 layer provides a good interface with AlGaIn/GaN, as the HEMT devices made from it showed a high $I_{\text{on}}/I_{\text{off}}$ ratio of over 10^8 and a low subthreshold slope of 75 mV/dec. The UV/ NH_4OH surface treatment was found to be critical for achieving these excellent figures. While bare Sc_2O_3 suffers

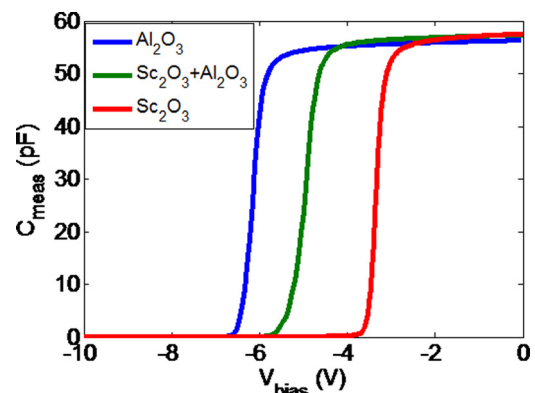


FIG. 6. Varying the Al_2O_3 percentage can be effective for changing the carrier concentration in the HEMT structure. Sc_2O_3 capacitor shown is measured in vacuum in order to avoid the impact of moisture. All C-V measurements were done at 1 MHz.

from moisture degradation, depositing a moisture blocking layer of ALD Al_2O_3 can effectively eliminate this effect. The Sc_2O_3 dielectric is found to be negatively charged, which facilitates the enhancement-mode operation.

We would like to acknowledge Professor Paul McIntyre and Dr. Rathnait Long at Stanford University for useful discussions about wet-treatments of AlGaIn/GaN HEMTs. This work was supported by the Office of Naval Research (ONR) under contract number ONR N00014-10-1-0937. This work was performed in part at the Center for Nanoscale Systems (CNS) at Harvard University, a member of the National Nanotechnology Infrastructure Network (NNIN), which is supported by the National Science Foundation under NSF Award No. ECS-0335765 and at the MIT Microsystems Technology Laboratory. The Lincoln Laboratory portion of this work was sponsored by the Department of Energy under Air Force Contract #FA8721-05-C-0002. The opinions, interpretation, conclusions, and recommendations are those of the authors and are not necessarily endorsed by the United States Government.

¹R. Mehandru, B. Luo, J. Kim, F. Ren, B. P. Gila, A. H. Onstine, C. R. Abernathy, S. J. Pearton, D. Gotthold, R. Birkhahn, B. Peres, R. Fitch, J. Gillespie, T. Jenkins, J. Sewell, D. Via, and A. Crespo, *Appl. Phys. Lett.*

- 82**(15), 2530 (2003); A. Y. Polyakov, N. B. Smirnov, A. V. Govorkov, V. N. Danilin, T. A. Zhukova, B. Luo, F. Ren, B. P. Gila, A. H. Onstine, C. R. Abernathy, and S. J. Pearton, *Appl. Phys. Lett.* **83**(13), 2608 (2003).
- ²J. J. Chen, B. P. Gila, M. Hlad, A. Gerger, F. Ren, C. R. Abernathy, and S. J. Pearton, *Appl. Phys. Lett.* **88**(14), 142115 (2006).
- ³A. M. Herrero, B. P. Gila, C. R. Abernathy, S. J. Pearton, V. Craciun, K. Siebein, and F. Ren, *Appl. Phys. Lett.* **89**(9), 092117 (2006); J. S. Jur, V. D. Wheeler, D. J. Lichtenwalner, J. P. Maria, and M. A. L. Johnson, *Appl. Phys. Lett.* **98**(4), 042902 (2011); X. Weng, W. Tian, D. G. Schlom, and E. C. Dickey, *Appl. Phys. Lett.* **96**(24), 241901 (2010).
- ⁴W. M. M. Kessels and M. Putkonen, *MRS Bull.* **36**(11), 907 (2011).
- ⁵P. de Rouffignac, A. P. Yousef, K. H. Kim, and R. G. Gordon, *Electrochem. Solid State Lett.* **9**(6), F45 (2006).
- ⁶M. Hong, A. R. Kortan, P. Chang, Y. L. Huang, C. P. Chen, H. Y. Chou, H. Y. Lee, J. Kwo, M. W. Chu, C. H. Chen, L. V. Goncharova, Garfunkel, and T. Gustafsson, *Appl. Phys. Lett.* **87**(25), 251902 (2005).
- ⁷M. M. Frank, Y. J. Chabal, and G. D. Wilk, *Appl. Phys. Lett.* **82**(26), 4758 (2003).
- ⁸Y. Liu, M. Xu, J. Heo, P. D. Ye, and R. G. Gordon, *Appl. Phys. Lett.* **97**(16), 162910 (2010).
- ⁹Y. Koyama, T. Hashizume, and H. Hasegawa, *Solid-State Electron.* **43**(8), 1483 (1999); R. D. Long and P. C. McIntyre, *Materials* **5**(7), 1297 (2012).
- ¹⁰O. I. Saadat and T. Palacios, in 2011 Proceedings of the European Solid-State Device Research Conference (ESSDERC), 12-16 September 2011, Helsinki (IEEE, New York, 2011), doi: 10.1109/ESSDERC.2011.6044178.
- ¹¹F. Gao, D. Chen, B. Lu, H. L. Tuller, C. V. Thompson, S. Keller, U. K. Mishra, and T. Palacios, *IEEE Electron. Device Lett.* **33**(10), 1378 (2012).
- ¹²P. F. Carcia, R. S. McLean, M. D. Groner, A. A. Dameron, and S. M. George, *J. Appl. Phys.* **106**(2), 023533 (2009).